PACS: 61.50.Ks, 71.15.Nc, 71.20.Lp

G.E. Grechnev[1,2], H.W. Hugosson[1], R. Ahuja[1], O. Eriksson[1]

STRUCTURAL EVOLUTION AND HARDNESS OF TRANSITION METAL DIOXIDES AT HIGH PRESSURE

[1]Condensed Matter Theory Group, Dept. of Physics, University of Uppsala
Box 534, S-751 21 Uppsala, Sweden

[2]B.I. Verkin Institute for Low Temperature Physics
47 Lenin's pr., Kharkov, 61164, Ukraine

There is a considerable amount of interest in the high-pressure phases of transition metal dioxides because these phases quite often exhibit high bulk moduli and thus are good candidates for hard materials. Here, we report the results of first-principles electronic structure calculations of the equation of state and volume-dependent bulk and electronic properties for a number of such oxides. A full-potential linear muffin-tin orbital method (LMTO) has been employed within the local density and general gradient approximations for exchange-correlation effects. The rutile-type and fluorite-type phases of these dioxides have been investigated. It was found that fluorite-type phases possess high bulk moduli, which is a result of a strong covalent bonding between d-states of transition metal and oxygen p-states. The possibility to stabilize these high-pressure phases at ambient conditions, for instance by epitaxial growth on a cubic substrate, could open new avenues for hard materials to be used in technological applications.

Introduction

In the last decade the search for candidates for new hard materials has been carried out experimentally, as well as theoretically, by employing new methods developed in computational solid-state physics. Initially this search was concentrated on covalent compounds, where directed covalent sp^3-bonds between atoms of C, B, and N can provide strong binding with a very rigid and hard structure, and the deformation of these bonds requires a substantial energy. Examples of such hard materials are diamond, the cubic BN, and the hexagonal WC [1–3]. Recently a new class of hard materials, namely transition metal dioxides MO_2, has been proposed [4–6]. Some phases of these compounds presumably possess high bulk moduli and therefore are candidates for hard materials.

A strong correlation between hardness and a bulk modulus value has been confirmed in a number of recent papers [1,7–9], indicating that the bulk modulus is related to the stiffness of the lattice. Strictly speaking, a high bulk modulus does not imply hardness in every case, and the shear moduli have to be high as well. Then a stress is not easily transferred in different directions, what prevents an unsymmetric distortion of the crystal lattice. Thus for noncubic compounds the shear moduli can serve as more reliable measure of the hardness, whereas for cubic compounds the bulk modulus should be a quite good indicator of hardness, since it is related to an isotropic deformation [4]. In the present work no attempts were made to obtain any quantitative values of hardness based on the calculated bulk moduli. The only assumption, used in evaluation whether a given compound is a good candidate for being

hard material, was a proportionality between hardness and stiffness.

Structural transitions have been observed in RuO_2 [4] from the rutile phase to an orthorhombic distorted rutile phase at a pressure of 8 GPa and then to the cubic fluorite phase at 12 GPa. This fluorite phase appeared to be metastable and having a very high bulk modulus, 399 GPa [4]. In order to reveal trends favourable for obtaining such hard materials, *ab initio* calculations of electronic structures and bulk properties are performed for a number of 4*d*- and 5*d*-transition metal dioxides. In this study we restrict our attention to dioxides with the ground state rutile (or distorted rutile) phase, and consider a possibility to stabilize the high-pressure cubic fluorite phase at ambient conditions.

Method of calculations

A full-potential linear muffin-tin orbital method [10] (FP-LMTO) has been employed to calculate the total energy as a function of volume for transition metal dioxides. The Kohn–Sham equation is solved for a general potential without any shape approximation. A unit cell is divided into non-overlapping muffin-tin spheres, surrounding each atomic site. Inside these spheres, where the charge density varies rapidly, the basis functions are Bloch functions built up of the radial functions times spherical harmonics. In the interstitial region, the charge density is slowly varying, and a basis function in the interstitial is defined by the Bloch function of solutions to the spherical Helmholtz equation with nonzero kinetic energy κ^2, or a linear combination of such solutions for different kinetic energies. A basis function in the interstitial is therefore expressed as a Bloch sum of Hankel or/and Neuman functions, which in turn is represented as a Fourier series. The Fourier representation of this basis function is taken from the Fourier series of a function matching the basis in the interstitial region but not inside the muffin-tin (MT) spheres, a so-called pseudowave function, whose exact shape inside the MT is of no principal importance for the final solution as long as it is continuous and differentiable at the sphere boundary and matches the true basis function in the interstitial. It must also have zero slope at the origin of each sphere.

The radial part of a basis function is constructed from the numerical solutions $\phi_L(E_V,r)$ of the radial Schrödinger equation in a spherical potential at the fixed energy E_V and their energy derivatives, $d\phi_L(E_V,r)/dE$. Here, the index L stands for a collection of quantum numbers: the principal quantum number n, the orbital quantum number l, the azimuthal quantum number m, and the kinetic energy κ^2. The tails of the basis function outside their parent spheres were linear combinations of Hankel or Neuman functions with nonzero kinetic energy. Further, a so called «double basis» has been adopted, where two different orbitals for the same principal and angular quantum number are connected at the sphere boundaries, in a continuous and differentiable way, to Hankel or Neuman functions with different kinetic energy κ^2 in the interstitial region. The spherical harmonic expansion of the charge density, potential, and basis functions were carried out up to a cutoff in angular momentum, $l = 8$.

The potential used for solving the radial Schrudinger equation is obtained from the charge density by solving Poisson's equation. The exchange-correlation potential was treated in both local density approximation (LDA) [11] and the generalized gradient

approximation (GGA) [12] of the density functional theory. In the present calculations the spin-orbit coupling was included at each variational step, although the calculations were carried out in the scalar-relativistic approximation as well. Together with the variational principle, this reduces the Kohn–Sham equation to a generalized eigenvalue equation, which can be solved by matrix diagonalization. In the first iteration, the overlapping atomic charge densities were taken. A new charge density is then constructed from the eigenvectors obtained through the variational procedure, and a new solution is obtained. The procedure can then be repeated until some criterion for self-consistency is met.

The electrons of the transition metal were divided into core, pseudo-valence and valence states. In the present calculations the basis set included the $4p$, $5s$, $5p$, and $4d$ orbitals for $4d$-transition metals, correspondingly the $5p$, $6s$, $6p$, and $5d$ orbitals for $5d$-metals, and also $2s$, $2p$, and $3d$ orbitals on the oxygen site. All states were contained in the same energy panel, with the low-lying p-orbitals on the metal site treated as a pseudo-valence states, i.e. as itinerant electrons but with considerably lower tail energies. In this way hybridization between the valence and pseudo-valence states is taken into account. The integration over the Brillouin zone was performed using the special point sampling and with a Gaussian smearing of 10 mRy. After achievement of self-consistency, the tetrahedron method was employed to get the density of states (DOS) on a fine energy mesh.

The electronic structure calculations were performed for a number of lattice parameters for both fluorite and rutile structures. The fluorite structure has a FCC Bravais lattice with a metal atom at (0,0,0) and two oxygen atoms positioned at (1/4,1/4,1/4) and (−1/4,−1/4,−1/4) in units of the lattice constant. The transition metal atom has an octahedral environment with eight oxygen atoms as nearest neighbours, while the oxygen atoms are positioned at a tetrahedral site with four metal atoms as nearest neighbours. In the tetragonal rutile structure, the metal atoms are positioned at (0,0,0) and at (1/2,1/2,1/2) sites while the four oxygen atoms occupy $\pm(u,u,0)$ and $\pm(u+1/2,1/2-u,1/2)$ sites, with a typical value of 0.3 for the internal parameter u. There are the oxygen octahedra surrounding each M atom. The experimental values of c/a and u parameters were fixed in our calculations, with the lattice parameter a varying in a wide range.

Results and discussion

For the rutile phase the calculated lattice parameters appeared to be in agreement with experimental ones to within 2%, which is a rather normal underestimation when LDA is used in combination with FP-LMTO method. A large part of this underestimation is therefore probably due to the overbonding tendency of LDA, which gives slightly overestimated bulk modulus. By contrast, the GGA approximation often overestimates the lattice constants when compared with experiment, and the bulk moduli become smaller than the LDA and the experimental ones. In this work, however, we are interested mainly in revealing of general trends in the calculated electronic structure and bulk moduli. Therefore we present results obtained within LDA, in order to compare them with earlier calculations, which were performed within the same approximation.

The bulk moduli were evaluated for both the rutile and fluorite phases from the calculated total energy E as a function of volume V, which was fitted to analytical parametrizations for the equation of state, such as the Murnaghan and recently proposed universal [13] equations. As an example, the evaluated equations of state for rutile and fluorite phases of RuO_2 are presented in Fig. 1. In this case the calculated $E(V)$ values were fitted to Murnaghan integrated equation of state. The universal equation [13] has given almost the same $E(V)$ curves and bulk moduli for all compounds studied. The bulk moduli, B, calculated within LDA are listed in Table. The effect of the spin-orbit coupling, included to the Hamiltonian, appeared to be almost negligible for the calculated bulk moduli, even for $5d$-transition metal dioxides.

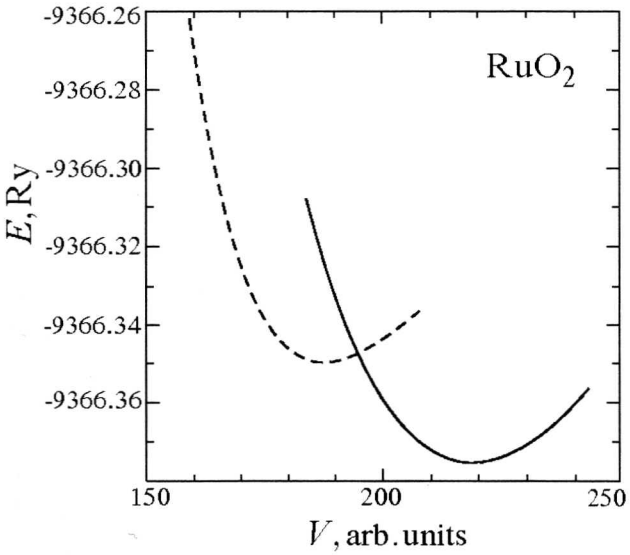

Fig. 1. The calculated equations of state for rutile (solid) and fluorite (dashed) phases of RuO_2 fitted to Murnaghan integrated equation. Energies and volume are given in atomic units per RuO_2 molecule

Table

Bulk moduli, B_{theory} and B_{exp}, of transition metal dioxides (in GPa). Lattice parameter, a_{theory}, in a.u.

Compound	Structure	a_{theory}	B_{theory}	B_{exp}
RuO_2	rutile	8.42	297	270
	fluorite	9.00	345	399
RhO_2	rutile	8.39	249	–
	fluorite	9.11	303	–
TcO_2	rutile	8.45	290	–
	fluorite	9.05	327	–
OsO_2	rutile	8.51	271	–
	fluorite	8.99	392	–
IrO_2	rutile	8.53	266	–
	fluorite	9.20	319	–
ReO_2	rutile	8.61	256	–
	fluorite	9.26	305	–
$ReRhO_4$	rutile	8.55	255	–
	fluorite	9.13	325	–

The electronic structure of MO_2 compounds is governed by a strong hybridization between the M-*d* and O-*p* states. The total densities of electronic states (DOS), $N(E)$, evaluated for fluorite and rutile phases of OsO_2, are presented in Fig. 2 and Fig. 3, respectively. For the corresponding phases of the isovalent compound RuO_2, the behaviour of $N(E)$ was found to be very similar. In general features this behaviour is reproduced qualitatively for other later dioxides: RhO_2, IrO_2, TcO_2, and ReO_2. As is seen in Fig. 2, the total DOS for the fluorite phase consists of four groups of bands, well resolved in energy. The two lowest are dominated by the O-*p* character with a small Os-*d* contribution, while the two higher lying bands are dominated by the Os-*d* states with a small fraction of the oxygen *p*-states. Therefore the two lowest groups of bands can be considered as the bonding part of the hybridization complex formed by the nearest neighbour bonding O-*p* and Os-$d_{t_{2g}}$ states, while the unoccupied highest lying bands belong to the corresponding anti-bonding part. The third highest lying occupied narrow peak is formed predominantly by the non-bonding Os-d_{e_g} states. In the fluorite phase RuO_2 and OsO_2, analogously to diamond, have an optimal number of valence electrons to occupy the bonding states, while leaving the anti-bonding states unoccupied. There is also an optimal energy separation between the O-*p* and metal *d*-states in these compounds to provide strong bonds without having to invoke any substantial charge transfer. The small charge transfer from oxygen to the bond between Ru (or Os) and O points to covalent character of the bonds.

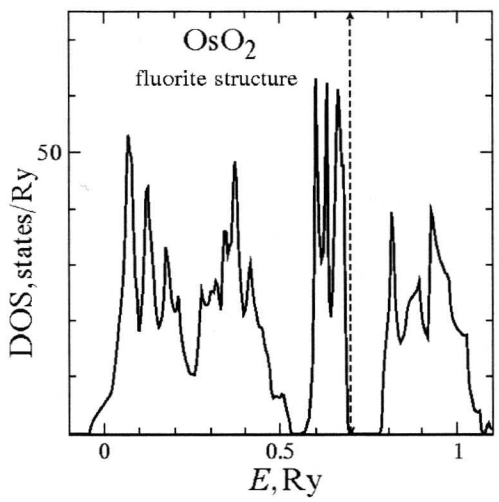

Fig. 2. The total density of states for OsO_2 in the fluorite phase

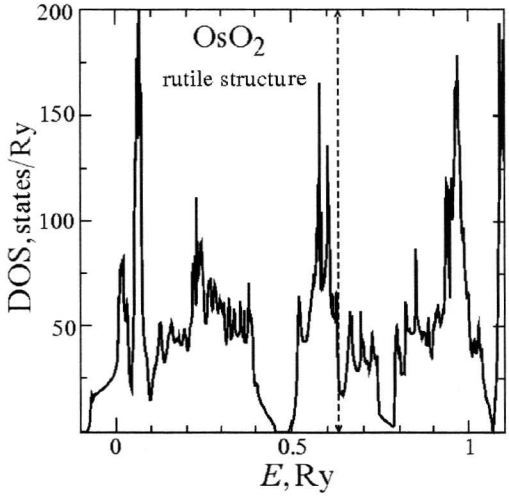

Fig. 3. The total density of states for OsO_2 in the rutile phase

The rutile phases of OsO_2 and RuO_2 are metallic, with the Fermi level positioned in a local minimum of $N(E)$ in Fig. 3. In general features this $N(E)$ resembles the DOS calculated for the fluorite structure (see Fig. 2), indicating a strong *p*–*d* hybridization. The high peak just below E_F originates mainly from the Os-$d_{t_{2g}}$ states, whereas the lower broad peaks lie in the range of predominantly oxygen *p*-states. There is a qualitative agreement of the calculated DOS in Fig. 3 with the experimental

XPS spectra measured for RuO_2 [14].

As can be seen in Table, changing from Ru to Os increased the bulk modulus for the fluorite phase of the dioxide. Substituting Ru (or Os) in the dioxides with a *d*-element from another group leads to larger equilibrium volumes and smaller bulk moduli. For later transition metals, Rh and Ir in MO_2, the anti-bonding states are getting filled leading, in turn, to weaker bonds. When going to lighter transition metals, Tc and Re in MO_2, the unfilling of the non-bonding d_{e_g} states has but little effect on the bonding properties. However, a high value of DOS at the Fermi energy indicates that the fluorite structure is probably unstable for TcO_2 and ReO_2. For the early $4d$- and $5d$-dioxides the bonds are of more ionic character.

Besides studying MO_2 compounds, the similar calculations were performed for a pseudo-binary dioxide with rutile-like ground state structure, namely $ReRhO_4$ [15]. The corresponding bulk moduli are given in Table, and appeared to be some lower than for isovalent RuO_2 and OsO_2 compounds both in the rutile and fluorite phases.

In summary, the electronic structure of transition metal dioxides in rutile and fluorite structures has been calculated and high bulk moduli were evaluated for MO_2 in the cubic fluorite phase, especially for the isovalent compounds RuO_2 and OsO_2. These results can be explained by specific favourable conditions for strong covalent bonds for these materials. The calculated electronic structure and bulk properties of RuO_2 are in good agreement with experiments. It seems promising to study a possibility to stabilize more dioxides in the cubic fluorite (or a fluorite-like) structure under high pressure, or at ambient conditions, for instance by epitaxial growth on a cubic substrate.

This project has been financed by the Swedish Natural Science Research Council (NFR and TFR).

1. *A.Y. Liu, R.M. Wentzcovich, M.L. Cohen*, Phys. Rev. **B38**, 9483 (1988).
2. *M.L. Cohen*, J. Hard Mater. **2**, 13 (1991).
3. *H.W. Hugosson, O. Eriksson, L. Nordstrom, U. Jansson, L. Fast, A. Delin, J.M. Wills, B. Johansson*, Phys. Rev. **B60**, 3758 (1999).
4. *J.M. Legŭr, B. Blanzat*, J. Mater. Sci. Lett. **13**, 1688 (1994).
5. *U. Lundin, L. Fast, L. Nordstrom, B. Johansson, J.M. Wills, O. Eriksson*, Phys. Rev. **B57**, 4979 (1998).
6. *J.E. Lowther, J.K. Dewhurst, J.M. Legŭr, J. Haines*, Phys. Rev. **B60**, 14485 (1999).
7. *M. Ashizuka, M. Murkami*, J. Japan Institute Metals **53**, 88 (1989).
8. *H. Neumann*, Cryst. Res. Tech. **23**, 97 (1988).
9. *C. Sung, M. Sung*, Mater. Chem. Phys. **43**, 1 (1996).
10. *J.M. Wills* (unpublished); *J.M. Wills, B.R. Cooper*, Phys. Rev. **B36**, 3809 (1987).
11. *U. von Barth, L. Hedin*, J. Phys. **C5**, 1629 (1972).
12. *J.P. Perdew, K. Burke, M. Ernzerhof*, Phys. Rev. Lett. **77**, 3865 (1996).
13. *P. Vinet, J.H. Rose, J. Ferrante, J.R. Smith*, J. Phys.: Condens. Matter **1**, 1941 (1989).
14. *R.R. Daniels, G. Margaritondo*, Phys. Rev. **B29**, 1813 (1984).
15. *I.S. Shaplygin, G.L. Arapnikov*, Rus. J. Inorgan. Chem. **32**, 624 (1987).